The discrete breast cancer stem cell mammosphere activity of Group 10-bis(azadiphosphine) metal complexes

Zhiyin Xiao,[a,b]‡ Alice Johnson,[a]‡ Kuldip Singh,[a] and Kogularamanan Suntharalingam [a]*

Dedication ((optional))

[a] Dr Z. Xiao, Dr A. Johnson, Dr K. Singh Dr K. Suntharalingam
School of Chemistry
University of Leicester
Leicester, UK
E-mail: k.suntharalingam@leicester.ac.uk
[b] Dr Z. Xiao
College of Biological, Chemical Sciences and Engineering
Jiaxing University
Jiaxing, China

‡ These authors contributed equally to this work

Supporting information for this article is given via a link at the end of the document.((Please delete this text if not appropriate))

Abstract: We report the anti-breast cancer stem cell (CSC) properties of a series of Group 10-bis(azadiphosphine) complexes **1**-**3** under exclusively three-dimensional cell culture conditions. The breast CSC mammosphere potency of **1**-**3** is dependent on the Group 10 metal present, increasing in the following order: **1** (nickel complex) < **2** (palladium complex) < **3** (platinum complex). Notably, **3** reduces the formation and size of mammospheres to a greater extent than salinomycin, an established CSC-active compound, or any reported anti-CSC metal complex tested under similar conditions. Mechanistic studies suggest that the most effective complexes **2** and **3** readily penetrate CSC mammospheres, enter CSC nuclei, induce genomic DNA damage, and trigger caspase-dependent apoptosis. To the best of our knowledge, this is the first study to systematically probe the anti-CSC activity of a series of structurally related Group 10 complexes and to be conducted entirely using three-dimensional CSC culture conditions.

Introduction

The platinum drugs cisplatin, carboplatin, and oxaliplatin, are routinely used in frontline cancer therapy.[1] They are estimated to be administered to half of all cancer patients at some point during their treatment regimens.[2] However, cisplatin, carboplatin, and oxaliplatin are unable to remove a small subpopulation of tumour cells called cancer stem cells (CSCs), at their clinically administered doses.[3] This is critical as CSCs are heavily linked to tumour relapse and metastasis, which are the leading causes of cancer associated deaths.[4] CSCs can self-renew, differentiate, and form secondary tumours.[5] CSCs are also chemo- and radiation-therapy resistant and thus can survive conventional anticancer approaches (including platinum therapy) and instigate secondary tumours with high metastatic fidelity.[6] Therefore, to improve clinical outcomes, it is vital that treatments have the ability to eradicate the entire population of cancer cells, including CSCs, otherwise CSC-mediated relapse and metastasis could occur.

The ineffectiveness of DNA-damaging platinum drugs against CSCs is likely due to their high capacity for DNA repair, high expression of drug-efflux pumps, and slow rate of division.[7] Several biological studies have shown that cisplatin, carboplatin, and oxaliplatin all enrich CSCs in heterogeneous tumour populations.[8] Although efforts are underway to develop platinum agents that can remove bulk cancer cells and CSCs at clinically relevant concentrations, only one platinum(II) complex, *trans*-[$PtCl_2$(2-(2-hydroxyethyl)pyridine)$_2$], and three platinum(IV) complexes, *cis*,*trans*,*cis*-[$Pt(NH_3)_2(OH)$(cinnamic acid)Cl_2], *cis*,*trans*,*cis*-[$Pt(NH_3)_2$(cinnamic acid)$_2Cl_2$] and *cis*,*trans*,*cis*-[$Pt(NH_3)_2$(*t*-cinnamate)(oleate)Cl_2], have been identified to effectively reduce the viability of (breast and rhabdomyosarcoma) CSCs *in vitro* (in the micro- or submicro-molar range).[9] The lack of CSC-active and -selective platinum compounds has enticed research, albeit limited, into the anti-CSC properties of other Group 10 metal (palladium and nickel) complexes. In this context, a monocationic, square-planar palladium(II)-terpyridine complex with a saccharinate counter anion was reported to effectively kill prostate CSCs *in vitro* (in micromolar range).[10] A series of nickel(II)-phenanthroline complexes bearing dithiocarbamate ligands and a chiral metallo-supramolecular cylinder made up of three bis(pyridylimine) ligands wrapped in a helical fashion around two nickel(II) ions, displayed breast CSC-selective toxicity (in the micromolar range).[11] Encouragingly, for the supramolecular di-nickel(II) complex, *in vivo* studies showed that the *P*-enantiomer could reduce tumorigenesis of breast CSCs.[11b]

Despite the growing interest in the anti-CSC properties of Group 10 metal complexes, a holistic understanding of their anti-CSC potential is unknown. This is partly because the nickel, palladium, and platinum complexes that have been tested in CSC systems thus far differ vastly in their chemical structures, making comparisons based on the Group 10 metal difficult. Here we have sought to shed light on this knowledge space by comparing the anti-CSC properties of square-planar, cationic nickel(II), palladium(II), and platinum(II) complexes with two azadiphosphine ligands, **1**-**3** (Figure 1A). The azadiphosphine ligand was selected as it is known to form stable coordination complexes with group 10 metals through the formation of Ni/Pd/Pt-P bonds.[12] The azadiphosphine ligand was

functionalised with a hexyl hydrocarbon chain to endow reasonable lipophilicity and thus encourage CSC uptake. The two counter anions in each case were tetrafluoroborate. Therefore **1**-**3** are structurally analogous and differ only by the identity of the metal centre.

The complex designs of **1**-**3** are similar to previously reported four-coordinate gold(I) complexes with bidentate pyridyl phosphine ligands that have a broad spectrum of anticancer properties.[13] Within this class of anticancer agents, $[Au^{I}(bis(diphenylphosphino)ethane)_2]^+$ was identified as a frontrunner.[14] The gold(I) complex displayed highly promising *in vivo* activity against a range of murine solid and liquid tumours.[14] Notably, unlike most biologically-active gold(I) complexes, this complex was kinetically stable in solution and resistant to substitution reactions with physiologically relevant thiols.[14] Detailed mechanistic studies suggested that $[Au^{I}(bis(diphenylphosphino)ethane)_2]^+$ mainly induced mitochondrial dysfunction, possibly by acting as a uncoupler of oxidative phosphorylation.[15] The mechanism of cytotoxicity of $[Au^{I}(bis(diphenylphosphino)ethane)_2]^+$ was also associated to DNA strand-breaks, formation of DNA-protein cross-links, and the inhibition of protein synthesis.[15] Unfortunately, during the preclinical development of the gold(I) complex, it was found to be highly toxic to isolated rat and canine hepatocytes and rabbit myocytes.[16] Furthermore, the gold(I) complex was highly hepatotoxic in male beagle dogs and cardiotoxic in rabbits,[15-16] which curtailed its therapeutic application as an antitumor agent.

Results and Discussion

The Group 10-bis(azadiphosphine) complexes **1**-**3** were synthesised as outlined in Figure 1A. The azadiphosphine ligand, **L^1**, was prepared by reacting *n*-hexylamine with two equivalents of chlorodiphenylphosphine in the presence of trimethylamine, in DCM for 16 h. **L^1** was isolated in a good yield (81%) as a white solid, and fully characterized by ^{1}H, ^{13}C, and ^{31}P NMR, UV-vis and infrared spectroscopy, ESI mass spectrometry, and elemental analysis (see ESI, Figures S1-6). The nickel(II) and palladium(II) complexes, **1** and **2** were prepared by reacting **L^1** with 0.5 equivalents of the appropriate salt, $[Ni(H_2O)_6](BF_4)_2$ or $[Pd(NCMe)_4](BF_4)_2$, in DCM:MeCN or DCM, respectively. The platinum(II) complex, **3** was synthesised by reacting **L^1** with the appropriate equivalents of $[Pt(1,5\text{-cyclooctadiene})Cl_2]$ and $NaBF_4$ in DCM:MeOH. The complexes, **1**-**3** were isolated in good yields (86-89%) as yellow (**1** and **2**) or white (**3**) solids and characterised by ^{1}H, ^{13}C, ^{19}F, and ^{31}P NMR, UV-vis and infrared spectroscopy, ESI mass spectrometry, and elemental analysis (see ESI, Figures S6-24). Single crystals of **1**-**3** suitable for X-ray diffraction studies were obtained by layer-diffusion of hexane into a DCM solution of **1**-**3** (CCDC 2035446-2035448, Figure 1B and Table S1). Selected bond distances and bond angles data are presented in Tables S2-4. The cationic structures of **1**-**3** all consist of the Group 10 metal(II) bound to four phosphorous atoms belonging to two azadiphosphine ligands. As expected the P–M–P bite angle (where M = Group 10 metal) corresponding to phosphorus atoms within the same azadiphosphine ligand (73.32(5)° for **1**, 69.32(2)° for **2**, 69.83(7)° for **3**) is considerably smaller than the P–M–P angle associated to phosphorous atoms on different azadiphosphine ligands (106.68(5)° for **1**, 110.68(2)° for **2**, 110.17(7)° for **3**). The average P–M–P angles suggest that **1**-**3** adopt pseudo square-planar structures. The average Ni–P (2.18 Å), Pd–P (2.31 Å), and Pt–P (2.30 Å) bond distances are consistent with bond parameters for related complexes.[12]

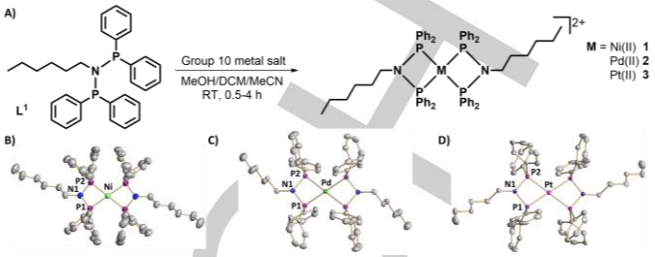

Figure 1. (A) Chemical reaction to form the Group 10-bis(azadiphosphine) complexes **1**-**3** using the azadiphosphine ligand, **L^1** and the appropriate Group 10 metal salt. The two counter anions for **1**-**3** are tetrafluoroborate. (B-D) X-ray structures of **1**-**3** comprising of two **L^1** ligands and the corresponding Group 10 metal(II) ion. Thermal ellipsoids are drawn at 30% probability. The hydrogen atoms, co-crystallizing solvent molecules (if any), and the tetrafluoroborate counter anions have been omitted for clarity.

The lipophilicity of **1**-**3** was determined by measuring the extent to which it partitioned between octanol and water, P. The experimentally determined Log P values varied from 0.15 to 0.36 (Table S5). The amphiphilic nature of **1**-**3** suggests that the complexes should be readily taken up by cells and soluble in aqueous solutions. Time course $^{31}P\{^1H\}$ NMR spectroscopy and ESI mass spectrometry studies were carried out to assess the stability of **1**-**3** in solution. The $^{31}P\{^1H\}$ NMR spectra for the palladium(II) and platinum(II) complexes, **2** (1 mM) and **3** (1 mM) in DMSO-d_6 displayed a single signal throughout the course of 72 h (at 45.03 ppm for **2** and 39.35 ppm for **3**) corresponding to the intact complexes (Figures S25-26). In contrast, the $^{31}P\{^1H\}$ NMR spectra for the nickel(II) complex, **1** in DMSO-d_6 displayed multiple signals over the course of 72 h (Figure S27). The signal for intact **1** (at 55.13 ppm) completely disappeared after 24 h, and was replaced by signals corresponding to **L^1** and its oxidised analogues, **L^{1}O** and **L^{1}OO**, indicative of solution instability (see Figures S28 for chemical structures and NMR signals in DMSO-d_6). **L^{1}O** and **L^{1}OO** were independently prepared and characterised by reacting **L^1** with the appropriate equivalents of H_2O_2 (see ESI) to confirm the abovementioned assignments (Figures S29-36). In H_2O:DMSO (200:1) the ESI

Table 1. IC_{50} values of the Group 10-bis(azadiphosphine) complexes **1**-**3**, the free azadiphosphine ligand **L^1**, salinomycin, cisplatin, and carboplatin against three-dimensional HMLER-shEcad mammospheres.

Compound	HMLER-shEcad mammosphere IC_{50} [μM][a]
1	2.98 ± 0.03
2	0.97 ± 0.09
3	0.24 ± 0.02
L^1	> 133
salinomycin [b]	18.50 ± 1.50
cisplatin [b]	13.50 ± 2.34
carboplatin [b]	18.06 ± 0.40

[a] Determined after 5 days incubation (mean of three independent experiments ± SD). [b] Reported in references 14.

mass spectra (positive mode) of the palladium(II) and platinum(II) complexes, **2** and **3** (50 μM) exhibited distinctive peaks corresponding to the intact complexes, with the expected isotopic pattern, throughout the course of 72 h at 37 °C (*m*/*z* = 522 a.m.u., [**2**-2BF$_4$]$^{2+}$; 566 a.m.u., [**3**-2BF$_4$]$^{2+}$) (Figures S37-38). The ESI mass spectra of the nickel(II) complex, **1** (50 μM) under the same conditions was dominated by a distinctive peak corresponding to **L^{1}OO** (*m*/*z* = 524 a.m.u., [**L^{1}OO**+Na]$^+$ (Figures S39). Taken together, the NMR spectroscopy and ESI mass spectrometry studies suggests that in solution (over 72 h), **1** decomposes to **L^1** (with the possible release of the nickel(II) ion), and the free ligand is subsequently oxidised to **L^{1}OO** (via **L^{1}O**) (Figures S40). These studies also clearly show that the palladium(II) and platinum(II) complexes, **2** and **3** are more stable than the nickel(II) complex **1** in solution.

The ability of the Group 10 metal complexes, **1**-**3** to inhibit the formation of spheroids comprising of breast CSCs was investigated using the mammosphere assay. Breast CSCs have the ability to form multicellular three-dimensional structures called mammospheres in serum-free, anchorage-independent cell cultures.[17] The mammosphere assay serves as a reliable readout for CSC potency and clinical potential, given that three-dimensional systems are more representative of solid tumours compared to more commonly used monolayer cell cultures. The addition of **1**-**3** (at the IC$_{20}$ value, determined from monolayer cytotoxicity studies, see ESI) to single cell suspensions of HMLER-shEcad cells significantly (p < 0.05) reduced the number and size of mammospheres formed after 5 days incubation (Figures 2A-B). The mammosphere inhibitory effect (according to the size and number of mammospheres formed) increased in the following order: **1** < **2** < **3**. This suggests that the mammosphere inhibitory effect of **1**-**3** is linked to the Group 10 metal present. The platinum(II) complex **3**, displayed the highest inhibitory effect, reducing the number of mammospheres formed by 92% compared to the untreated control. The mammosphere inhibitory effect of **3** was significantly greater than that of salinomycin, an established mammosphere-potent agent (Figures 2A-B) or any reported anti-CSC metal complex, under identical conditions.[18] Dosage with **L^1** (at 133 μM for 5 days) did not significantly (p = 0.22) reduce the number or size of mammosphere formed (Figures 2A-B), indicating that the Group 10 metal plays an important role in the mammosphere inhibitory effect of **1**-**3**.

Having proven that **1**-**3** are able to inhibit mammosphere formation, we investigated their ability to affect viability (metabolic activity). This is an important consideration as the reduction in the number and size of mammospheres formed does not necessarily mean that the mammospheres are no longer viable. To assess the ability of **1**-**3** to reduce mammosphere viability, the colorimetric resazurin-based reagent, TOX8 was used. TOX8 has been previously proven to be a suitable reagent for determining tumour spheroid viability.[19] The IC$_{50}$ values, the concentration required to reduce mammosphere viability by 50%, were determined from dose-response curves (Figure 2C) and are summarised in Table 1. The mammosphere potency of **1**-**3** were in the micro- or submicro-molar range. Alike the mammosphere formation inhibitory effect, the mammosphere potency of the metal complexes is discrete, and increased in the following order: **1** (IC$_{50}$ value = 2.98 ± 0.03 μM) < **2** (IC$_{50}$ value = 0.97 ± 0.09 μM) < **3** (IC$_{50}$ value = 0.24 ± 0.02 μM) (Figures 2C). This implies that the cytotoxicity of the Group 10-bis(azadiphosphine) complexes toward breast CSC spheroids is dependent on the Group 10 metal present. Strikingly, the platinum(II) complex, **3** displayed 77-, 56-, and 75-fold greater potency for mammospheres than salinomycin, cisplatin, and carboplatin, respectively under identical conditions. Unsurprisingly **L^1** was non-toxic towards mammospheres (IC$_{50}$ > 133 μM, Figures 2C and Table 1). This shows that the Group 10 metal in **1**-**3** is a major determinant of mammosphere toxicity. Collectively, the mammosphere studies show that the Group 10-bis(azadiphosphine) complexes, in particular the platinum(II) complex **3**, are able to markedly reduce breast CSC mammosphere formation, size, and viability. Reflecting on the abovementioned solution-stability results in light of the CSC mammosphere potency data, it is evident that stability bestows higher CSC mammosphere potency (within this family of complexes).

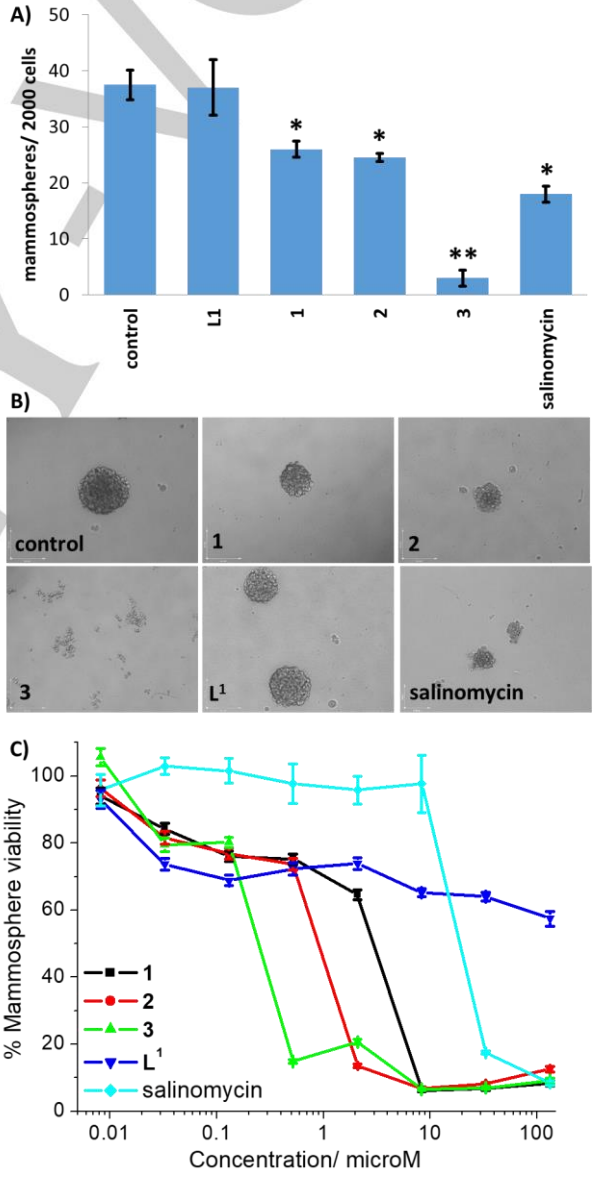

Figure 2. (A) Quantification of mammosphere formation with HMLER-shEcad cells untreated and treated with **1**-**3** or salinomycin at their respective IC$_{20}$ values, or **L^1** at 133 μM for 5 days. Error bars = SD and Student t-test, * = p < 0.05, ** = p < 0.01. (B) Representative bright-field images (x 10) of the mammospheres in the absence and presence of **1**-**3** or salinomycin at their respective IC$_{20}$ values, or **L^1** at 133 μM for 5 days. (C) Representative dose-response curves for the treatment of HMLER-shEcad mammospheres with **1**-**3**, **L^1** or salinomycin after 5 days incubation. Error bars = SD.

To provide insight into the mechanism of CSC mammosphere potency of **2** and **3** (the most effective and stable complexes within the series), further three-dimensional spheroid-based studies were carried out. Uptake studies were conducted to determine mammosphere permeability and CSC localisation. HMLER-shEcad mammospheres were treated with **2** and **3** at a non-lethal dose (1 μM for 6 h) and the palladium or platinum content was determined by inductively coupled plasma mass spectrometry (ICP-MS). The palladium(II) and platinum(II) complexes, **2** and **3** were readily taken up by HMLER-shEcad mammospheres, with mammosphere uptake totalling 6.98 ± 0.34 ng of Pd/ 10^3 mammospheres for **2** and 7.88 ± 0.21 ng of Pt/ 10^3 mammospheres for **3** (Figure 3A). Fractionation studies showed that a substantial amount of **2** and **3** entering HMLER-shEcad cells (making up mammospheres) was found in the nucleus (69% for **2** and 74% for **3**) providing remarkable access to genomic DNA (Figure 3A). Markedly lower amounts of internalised **2** and **3** were detected in the cytoplasm (10% for **2** and 12% for **3**) and membrane (16% for **2** and 10% for **3**) (Figure 3A). The cellular uptake data strongly suggests that **2**- and **3**-induced CSC mammosphere potency could be related to genomic DNA damage.

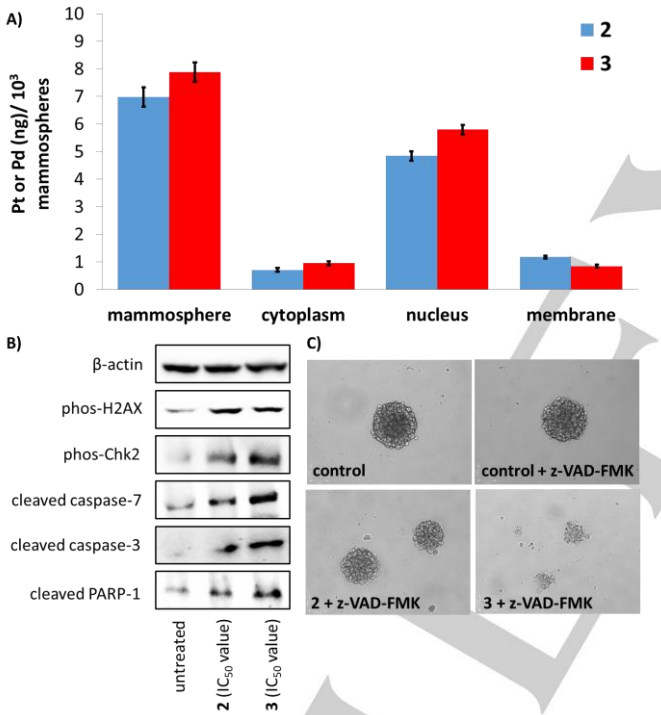

Figure 3. (A) Palladium or platinum content in mammosphere, cytoplasm, nucleus, and membrane fractions isolated from HMLER-shEcad mammospheres treated with **2** or **3** (1 μM for 6 h). Error bars = SD. (B) Immunoblotting analysis of proteins related to the DNA damage and apoptosis pathways. Protein expression in HMLER-shEcad mammospheres following treatment with **2** or **3** (IC_{50} value for 72 h). (C) Representative bright-field images (x 10) of the mammospheres in the absence and presence of **2** or **3** with z-VAD-FMK (5 μM) at their respective IC_{20} values for 5 days.

Given that **2** and **3** have access to nuclei within HMLER-shEcad mammospheres, their ability to induce DNA damage was studied by monitoring the expression of proteins related to the DNA damage pathway. Immunoblotting studies showed that HMLER-shEcad mammosphere treated with **2** or **3** (IC_{50} value for 72 h) displayed a marked increase in the expression of the phosphorylated form of H2AX and Chk2 indicative of DNA damage (Figure 3B).[20] As the palladium(II) and platinum(II) centres in **2** and **3**, respectively, are bound to strongly coordinating ligands and given their stability in solution, the complexes are unlikely to interact with DNA in a covalent manner. To determine the non-covalent binding affinity and mode of **2** and **3** to DNA, ethidium bromide (a strong intercalator) displacement studies were carried out. Upon incremental addition of **2** or **3** (0 - 100 μM) to a solution of ct-DNA (20 μM) and ethidium bromide (1 μM), the emission associated to the ethidium bromide-DNA complex (originating from the intercalation of ethidium bromide between DNA base pairs) markedly decreased (Figure S41-44). The quenching constants for **2** (K_q = 4.48 ± 0.48 × 10^5 M^{-1}) and **3** (K_q = 1.46 ± 0.11 × 10^5 M^{-1}) were comparable to those reported for moderate metallointercalators suggesting that **2** and **3** can bind to DNA via intercalation (most likely via the phenyl groups on $\mathbf{L^1}$).[21] DNA intercalation could be the mechanism by which **2** and **3** induces DNA damage in CSCs. DNA damage can lead to caspase-dependent apoptosis.[22] Immunoblotting studies showed that HMLER-shEcad mammospheres treated with **2** or **3** (IC_{50} value for 72 h) displayed markedly higher levels of cleaved caspase 3 and 7, and poly-ADP ribose polymerase (PARP) compared to untreated cells (Figure 3B), suggestive of caspase-dependent apoptosis. Independent mammosphere studies in the presence of z-VAD-FMK (5 μM), a caspase-dependent apoptosis inhibitor clearly showed that the inhibitory effect of **2** and **3** (at the IC_{20} value after 5 days incubation) on HMLER-shEcad mammospheres formation was attenuated, in terms of the number, size, and spherical nature of mammospheres formed (Figures 3C and S45). Specifically, co-incubation with z-VAD-FMK (5 μM) decreased the ability of **2** to reduce the number of mammospheres formed from 33% to 16% compared to the appropriate control (a relative decrease of 52%) (Figure S45). At the same time, co-treatment with z-VAD-FMK (5 μM) decreased the ability of **3** to reduce the number of mammospheres formed from 92% to 48% compared to the appropriate control (a relative decrease of 48%) (Figure S45). Therefore for **2** and **3**, z-VAD-FMK had a markedly similar effect on their mammosphere inhibitory effect. The potency of **2** and **3** towards HMLER-shEcad mammospheres also decreased, albeit marginally, in the presence of z-VAD-FMK (IC_{50} value for **2** = 1.15 ± 0.04 μM and for **3** = 0.31 ± 0.01 μM) (Figure S46). Altogether, this suggests that **2** and **3** are likely to induce DNA damage and caspase-dependent CSC mammosphere death.

Conclusion

In summary, we report the varying breast CSC activities of a new series of Group 10-bis(azadiphosphine) complexes, **1**-**3** under exclusively three-dimensional cell culture conditions. The CSC mammosphere potency of **1**-**3** was dependent on the Group 10 metal present, increasing 'down the group' in the following order: **Ni** < **Pd** < **Pt**. It is conceivable that the Group 10 metal atom solely plays a role in determining the stability of the complex and consequently the CSC mammosphere activity of the complex. Despite the similar solution stabilities of **2** and **3**, the complexes could have different reactivity towards biological nucleophiles which will impact their CSC mammosphere potency. From our results, it is clear that the platinum(II) complex **3** displays markedly higher CSC mammosphere potency than the nickel(II) complex **1** and the palladium(II) complex **2**. This result

could be related to the relative facile deactivation of **1** or **2** by unwanted side-reactions with biological nucleophiles, compared to **3**, given the inherent differences in biological stabilities of related nickel(II), palladium(II), and platinum(II) complexes. Strikingly, the most effective complex, **3**, displayed 56-77 times higher potency for CSC mammospheres than salinomycin, cisplatin, and carboplatin. The solution stable platinum(II) and palladium(II) complexes, **2** and **3** induce CSC mammosphere toxicity by penetrating CSC mammospheres in reasonable amounts, entering the nuclei of CSCs making up the mammospheres, inflicting genomic DNA damage, and prompting caspase-dependent apoptosis. Our findings reinforce the therapeutic potential of Group 10 metal complexes and provide fresh impetus for their development as anti-CSC agents.

Acknowledgements ((optional))

K.S. is supported by an EPSRC New Investigator Award (EP/S005544/1). Z.X. thanks the National Natural Science Foundation of China (21807047) for financial support.

Keywords: Group 10 • antitumour agents • DNA damage • cancer stem cell • mammosphere

[1] T. C. Johnstone, K. Suntharalingam, S. J. Lippard, *Chem. Rev.* **2016**, *116*, 3436-3486.
[2] M. Galanski, M. A. Jakupec, B. K. Keppler, *Curr. Med. Chem.* **2005**, *12*, 2075-2094.
[3] F. Tomao, A. Papa, L. Rossi, M. Strudel, P. Vici, G. Lo Russo, S. Tomao, *J. Exp. Clin. Cancer Res.* **2013**, *32*, 48.
[4] L. V. Nguyen, R. Vanner, P. Dirks, C. J. Eaves, *Nat. Rev. Cancer* **2012**, *12*, 133-143.
[5] J. Marx, *Science* **2007**, *317*, 1029-1031.
[6] a) M. Dean, T. Fojo, S. Bates, *Nat. Rev. Cancer* **2005**, *5*, 275-284; b) D. R. Pattabiraman, R. A. Weinberg, *Nat. Rev. Drug Discov.* **2014**, *13*, 497-512.
[7] C. Gasch, B. Ffrench, J. J. O'Leary, M. F. Gallagher, *Mol. Cancer* **2017**, *16*, 43.
[8] a) L. Wang, X. Liu, Y. Ren, J. Zhang, J. Chen, W. Zhou, W. Guo, X. Wang, H. Chen, M. Li, X. Yuan, X. Zhang, J. Yang, C. Wu, *Cell Death Dis.* **2017**, *8*, e2746-e2746; b) K. Suntharalingam, W. Lin, T. C. Johnstone, P. M. Bruno, Y. R. Zheng, M. T. Hemann, S. J. Lippard, *J. Am. Chem. Soc.* **2014**, *136*, 14413-14416; c) C. Saygin, A. Wiechert, P. Thiagarajan, V. Rao, J. Hale, M. Hitomi, A. DiFeo, J. Lathia, O. Reizes, *J. Clin. Oncol.* **2016**, *34*, e17098-e17098; d) G. Bertolini, L. Roz, P. Perego, M. Tortoreto, E. Fontanella, L. Gatti, G. Pratesi, A. Fabbri, F. Andriani, S. Tinelli, E. Roz, R. Caserini, S. Lo Vullo, T. Camerini, L. Mariani, D. Delia, E. Calabro, U. Pastorino, G. Sozzi, *Proc. Natl. Acad. Sci. U.S.A.* **2009**, *106*, 16281-16286.
[9] a) N. Aztopal, D. Karakas, B. Cevatemre, F. Ari, C. Icsel, M. G. Daidone, E. Ulukaya, *Bioorg. Med. Chem.* **2017**, *25*, 269-276; b) J. Zajac, V. Novohradsky, L. Markova, V. Brabec, J. Kasparkova, *Angew. Chem. Int. Ed.* **2020**, *59*, 3329-3335; c) H. Kostrhunova, J. Zajac, L. Markova, V. Brabec, J. Kasparkova, *Angew. Chem. Int. Ed.*, DOI: 10.1002/anie.202009491.
[10] E. Ulukaya, F. M. Frame, B. Cevatemre, D. Pellacani, H. Walker, V. M. Mann, M. S. Simms, M. J. Stower, V. T. Yilmaz, N. J. Maitland, *PloS one* **2013**, *8*, e64278.
[11] a) M. Flamme, P. B. Cressey, C. Lu, P. M. Bruno, A. Eskandari, M. T. Hemann, G. Hogarth, K. Suntharalingam, *Chemistry* **2017**, *23*, 9674-9682; b) H. Qin, C. Zhao, Y. Sun, J. Ren, X. Qu, *J. Am. Chem. Soc.* **2017**, *139*, 16201-16209.
[12] a) Z. Xiao, M. Natarajan, W. Zhong, X. Liu, *Electrochim. Acta* **2020**, *340*, 135998; b) C. Fliedel, V. Faramarzi, V. Rosa, B. Doudin, P. Braunstein, *Chem. Eur. J.* **2014**, *20*, 1263-1266; c) T. Tanase, M. Tanaka, M. Hamada, Y. Morita, K. Nakamae, Y. Ura, T. Nakajima, *Chem. Eur. J.* **2019**, *25*, 8219-8224.
[13] S. J. Berners-Price, A. Filipovska, *Metallomics* **2011**, *3*, 863-873.
[14] S. J. Berners-Price, C. K. Mirabelli, R. K. Johnson, M. R. Mattern, F. L. McCabe, L. F. Faucette, C. M. Sung, S. M. Mong, P. J. Sadler, S. T. Crooke, *Cancer Res.* **1986**, *46*, 5486-5493.
[15] M. J. McKeage, L. Maharaj, S. J. Berners-Price, *Coord. Chem. Rev.* **2002**, *232*, 127-135.
[16] a) G. D. Hoke, R. A. Macia, P. C. Meunier, P. J. Bugelski, C. K. Mirabelli, G. F. Rush, W. D. Matthews, *Toxicol. Appl. Pharmacol.* **1989**, *100*, 293-306; b) P. F. Smith, G. D. Hoke, D. W. Alberts, P. J. Bugelski, S. Lupo, C. K. Mirabelli, G. F. Rush, *J. Pharmacol. Exp. Ther.* **1989**, *249*, 944-950.
[17] G. Dontu, W. M. Abdallah, J. M. Foley, K. W. Jackson, M. F. Clarke, M. J. Kawamura, M. S. Wicha, *Genes Dev.* **2003**, *17*, 1253-1270.
[18] a) K. Laws, G. Bineva-Todd, A. Eskandari, C. Lu, N. O'Reilly, K. Suntharalingam, *Angew. Chem. Int. Ed.* **2018**, *57*, 287-291; b) J. N. Boodram, I. J. McGregor, P. M. Bruno, P. B. Cressey, M. T. Hemann, K. Suntharalingam, *Angew. Chem. Int. Ed.* **2016**, *55*, 2845-2850; c) A. Eskandari, A. Kundu, S. Ghosh, K. Suntharalingam, *Angew. Chem. Int. Ed.* **2019**, *58*, 12059-12064.
[19] R. Mezencev, L. Wang, J. F. McDonald, *J. Ovarian Res.* **2012**, *5*, 30.
[20] a) E. P. Rogakou, D. R. Pilch, A. H. Orr, V. S. Ivanova, W. M. Bonner, *J. Biol. Chem.* **1998**, *273*, 5858-5868; b) J. Y. Ahn, J. K. Schwarz, H. Piwnica-Worms, C. E. Canman, *Cancer Res.* **2000**, *60*, 5934-5936.
[21] R. Raj Kumar, M. K. Mohamed Subarkhan, R. Ramesh, *RSC Adv.* **2015**, *5*, 46760-46773.
[22] W. P. Roos, A. D. Thomas, B. Kaina, *Nat. Rev. Cancer* **2016**, *16*, 20-33.

Entry for the Table of Contents

Insert graphic for Table of Contents here. ((Please ensure your graphic is in **one** of following formats))

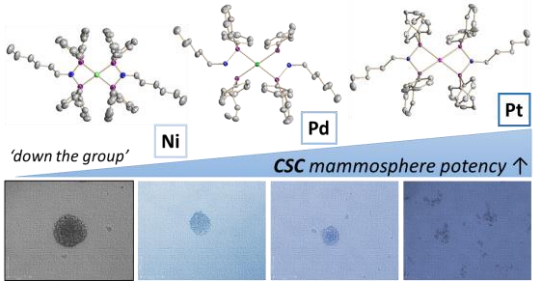

Killing cancer stem cells 'down the group'. Cancer stem cells (CSCs) are associated to cancer relapse and metastasis. Here we systematically compare the breast CSC activities of Group 10-bis(azadiphosphine) complexes under exclusively three-dimensional cell culture conditions. Breast CSC mammosphere inhibition and potency was highly dependent on the Group 10 metal present.

Institute and/or researcher Twitter usernames: @_Suntharalingam @Leicesterchem @LeicStructBio @uniofleicester